J. exp. Biol. **127**, 45–57 (1987)
Printed in Great Britain © *The Company of Biologists Limited 1987*

THE WAKE OF A KESTREL (*FALCO TINNUNCULUS*) IN GLIDING FLIGHT

BY G. R. SPEDDING*

Department of Zoology, University of Bristol, Woodland Road, Bristol BS8 1UG

Accepted 19 August 1986

SUMMARY

The wake of a kestrel gliding down a 36 m long corridor was examined using multiple-flash stereo photographs of small bubbles of helium in soap solution. Qualitatively and quantitatively, the wake is very similar to that which would be measured behind an elliptically loaded aerofoil of the same span. The significance of this close agreement with classical aerodynamic theory is briefly discussed and the results are compared with others measured or assumed in the bird flight literature.

INTRODUCTION

There have been a number of attempts to model aspects of bird flight of interest to both ecologists and aerodynamicists, aimed, on the one hand, at predicting the energetic cost of flight to the bird and attempting to understand its behaviour in this light (e.g. Pennycuick, 1969, 1978; Tucker, 1971; Greenewalt, 1975), and, on the other, trying to model with some degree of accuracy the unsteady or nonlinear terms in the aerodynamic model which arise as a consequence of the oscillation and/or irregular shape of the lifting surfaces (Lan, 1979; Phlips, East & Pratt, 1981). As can be readily appreciated from the above references, no model can be cast exclusively as one or other of these two types; energetic models, in order to be sufficiently general, make broad assumptions concerning the flow over the wings and the resulting aerodynamic forces, while the aerodynamic models must usually assume some simplified wing beat kinematics or wake geometry (Rayner, 1979*a*,*b*; Phlips *et al.* 1981). All models assume that the wings of a bird operate in the same fashion as a conventional aerofoil, with various degrees of unsteadiness (typically measured by the reduced frequency $\Omega = c\omega/2U$, where U is the freestream velocity, c is a streamwise length scale (such as the mean chord) and ω is the radian frequency of oscillation) caused by the flapping motion. In the limit of zero-reduced frequency, gliding flight, such an approach has met with some success in analysing the flight behaviour of large birds which depend on gliding as their primary means of transport

* Present address: Department of Aerospace Engineering, University of Southern California, University Park, Los Angeles, CA 90089–0192, USA.

Key words: kestrel, wake, flight.

(e.g. Pennycuick, 1971*a*,*b*, 1982). Flapping flight has also been studied in the light of model predictions (e.g. Pennycuick, 1975; Rayner, 1979*b*; Norberg, 1979) but the agreement with direct physiological measurements of oxygen consumption has been poor (Tucker, 1973; Torre-Bueno & Larochelle, 1978). In all cases, the model predictions assume, either implicitly or explicitly, that the wings behave as a conventional wing pair, operating at or near an optimum elliptical spanwise load distribution.

This paper is the first of two which use a previously reported flow visualization technique (Spedding, Rayner & Pennycuick, 1984) to analyse the wake of a bird flying at a moderate flight speed. The gliding flight results, reported here, enable some of the performance characteristics of the wings to be inferred from some simple wake measurements, and mark the first time that such results have been measured from a live, freely flying animal.

MATERIALS AND METHODS

Apparatus and experimental procedure

The apparatus was a portable version of that described by Spedding *et al.* (1984) and is shown schematically in Fig. 1. A rigid frame constructed of slotted angle iron (Dexion) supported a pair of 35 mm Nikon cameras in precisely defined positions so that the film planes were coplanar and equal in height from the floor and the lens axes were normal to this plane and parallel to each other. This frame was recessed in a doorway halfway down a 36 m corridor. Opposite the doorway a cloud of helium-filled soap bubbles was generated (Armstrong SAI Bubble Generator with Low Speed Head no. 2) in front of a plain dark background. A hand-trained kestrel was taught to fly from one operator (1) to another (2) at the opposite end of the corridor in order to receive his daily feed. The experiments were run at dusk for multiple-flash photography and around 10 flights could be elicited each evening. As the kestrel flew across the field of view of the cameras, operator 2 closed a switch, opening the camera shutters and triggering the sequential firing of a series of four flash guns with flash intervals determined accurately by a purpose-built timer.

In the first series of flights, as shown in Fig. 1, the kestrel quickly built up speed after leaving operator 1 (approx. 1 m above ground) and then, dropping to a flying height of about 40 cm, continued in a shallow glide before pulling up to land at operator 2, again about 1 m from the floor. Throughout the gliding phase, the wings were held fully outstretched with the primary feathers extended. Timed with a stopwatch, the average flight speed was $6\,m\,s^{-1}$ and, allowing for acceleration from rest and deceleration at the end of the flight, the flight speed in the middle portion of the flight, including the initial gliding phase in front of the cameras, was estimated at $7\,m\,s^{-1}$. These rather crude measures of the flight pattern were not checked by high-speed ciné film analysis owing to the limited time available for experiments, but should be sufficient for a first order analysis, bearing in mind the possible sources of

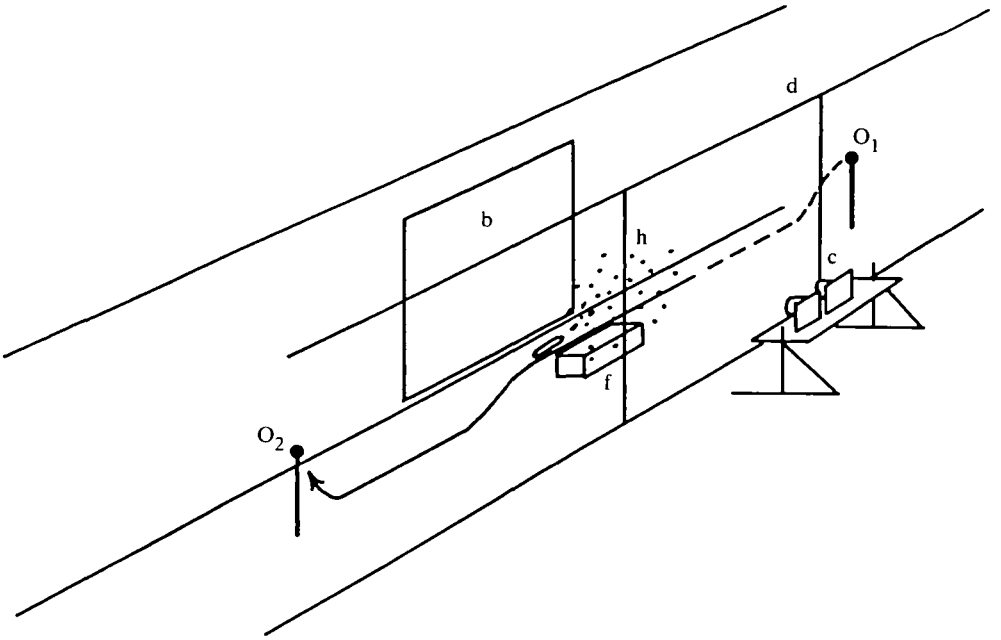

Fig. 1. The arrangement of the apparatus and operators 1 and 2 along a 36 m corridor. The flight path is approximately as shown by the dashed and solid lines. The kestrel took off from operator 1 (O_1), about 1 m from the ground, dropping to 300–400 mm and accelerating to 7 m s^{-1} in flapping flight. Gliding (solid line) commenced about 4–5 m before the flashguns (f) and continued at a shallow angle until 2 m or so past the flashguns. Once past this obstacle, the bird would drop closer to the floor before pulling up at a steep angle to decelerate and land on the wrist of O_2, again at a height of about 1 m. The cameras, c, are recessed in a doorway, d, facing a cloud of helium bubbles, h, which are generated in front of a dark background, b.

error. Both the flight height and the flight speed through the bubbles may be checked directly from the multiple flash photographs.

Photogrammetry

A right-handed coordinate system is defined with X and Y parallel and normal to the direction of flight, and Z parallel to the camera lens axes, and the u, v and w components of velocity in X, Y and Z are defined following the usual conventions, as shown in Fig. 2. From those stereopairs which showed the wake structure in gliding flight, one was subjected to a full stereophotogrammetric analysis, as described in Spedding *et al.* (1984). From the resulting three-dimensional velocity field, velocity profiles were taken in two-dimensional slices at appropriate locations across the wake and from these, estimates of the vorticity distribution and circulation of the vortices in the wake could be made.

Judging by an error analysis, as previously reported, together with reconstructions of a control object, it was estimated that velocities could be determined to within 13 %.

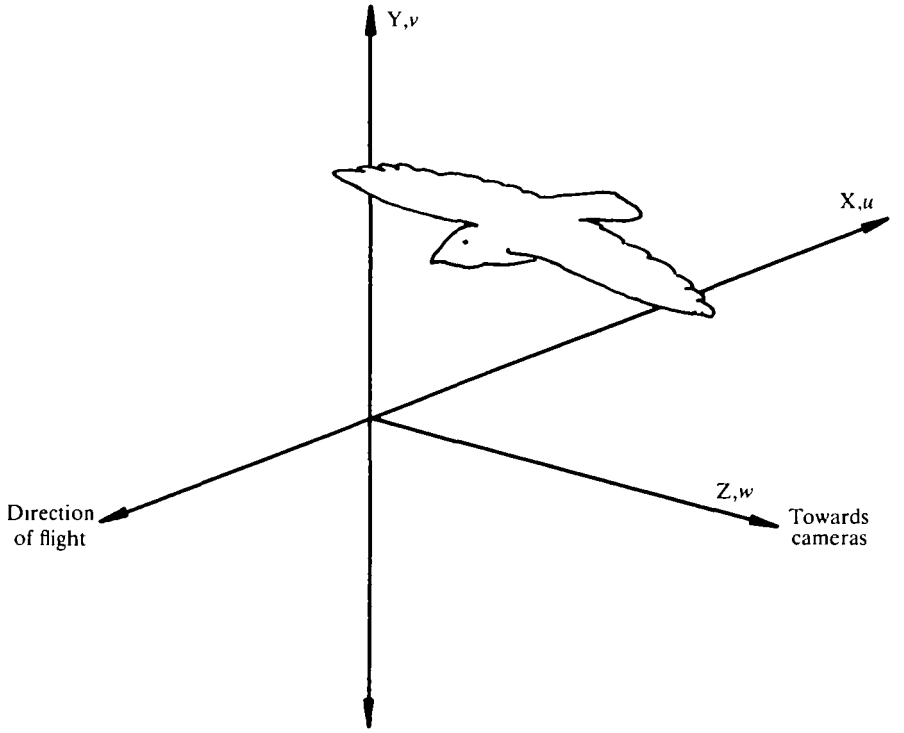

Fig. 2. Coordinate system and notation. The X, Y, Z coordinate system is fixed relative to the cameras with its origin (X_o, Y_o, Z_o) on the back wall, at the level of the left camera lens principal axis. Velocities are resolved into components u, v and w in the direction of X, Y and Z, respectively.

RESULTS

Fig. 3 is a stereopair of the wake behind a gliding kestrel. The tip of the tail is visible in stereo and may be used to locate the flight path. Behind the port wingtip (closest to the cameras) a line of bubbles circulating in a corkscrew type of motion can be seen stretching behind the bird, inclined at a small angle to the horizontal. This pattern is quite consistent with all the photographs examined and indicates the presence of a single pair of wingtip trailing vortices such as those observed behind fixed-wing aircraft. Assuming, for the moment, that their formation follows the classical pattern, roll-up of the unstable vortex sheet initially shed from the wing trailing edges appears to take place within 4–5 chord lengths. A sketch of the wake appears in Fig. 6.

A reconstruction of the bubble field is shown in Fig. 4, where the line of flight calculated from the tail tip position is indicated by the dashed line and numbered and lettered segments mark the location of vertical slices made in the YZ and XY planes, respectively. Three of these sections are shown in Fig. 5A–C. Fig. 5A and 5B cut along the edge of the vortex core, parallel to the line of flight, roughly at the inner and outer edges of the vortex, whilst Fig. 5C is a plane section normal to the long axis of

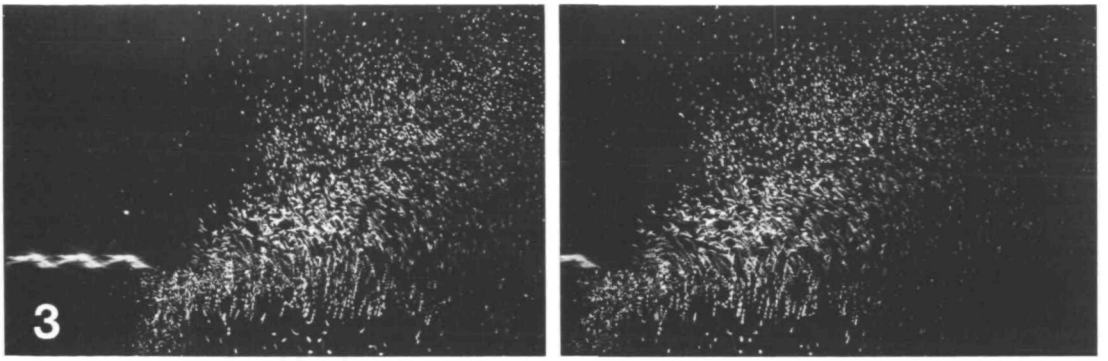

Fig. 3. The vortex wake of a gliding kestrel. In the foreground bubbles are circulating around a trailing vortex shed by the port wingtip. The mean delay between successive exposures is 16 ms.

the vortex. Fig. 6 is a schematic interpretation of the gliding wake from stereopairs such as Fig. 3, consistent with the qualitative analysis of these wake sections.

Serial reconstruction of the wake in this fashion allows the core centre in YZ to be estimated at each section. $w(Y)$ profiles were taken at a number of stations in Z, and Z_{core}, the Z location of the core centre, is that station with the greatest $|\partial w/\partial Y|$. At Z_{core}, Y_{core} is the location of maximum $|\partial v/\partial Z|$: The XZ location of the vortex core centre is plotted at seven downstream locations in Fig. 7. Slight oscillations of the wake vortices in Z may be discerned, but it is not clear whether this is due to limited experimental accuracy or to low-amplitude wing motions in flight. Measured from these data, the mean spanwise vortex separation, D, is $0{\cdot}513 \pm 0{\cdot}015$ m. Following roll-up, the diameter of the vortex core appeared to vary little with downstream distance in the wake, as far as could be told from the sparse data in some sections. The mean core diameter, d, was taken from the distance between w_{max} and w_{min} in a plot of $w(Y-Y_{core})$ for a number of downstream locations in the wake (Fig. 8). From this figure, the circulation, Γ, around the trailing vortex was estimated, assuming a circular core, from,

$$\Gamma = \pi d \cdot w_{max}. \tag{1}$$

DISCUSSION

Lifting-line theory

Classical aerofoil theory demonstrates that an optimum spanwise circulation distribution, in terms of minimizing the wake kinetic energy generated for a given amount of aerodynamic work, has the shape of a semi-ellipse for a fixed wing in steady flow. This wing loading distribution is reflected in the geometry of the wake and the results outlined above may be used for comparison. All quantities quoted for an elliptically loaded wing have been taken from Milne-Thompson (1966) in the following discussion.

Accordingly, the spanwise spacing between cylindrical vortices shed from an elliptically loaded wing is given by:

$$D = 2b\pi/4, \tag{2}$$

where b is the wing semispan. In dimensionless form, the wake spacing is the spanwise separation of the wingtip trailing vortices relative to the wingspan, 2b,

$$R' = D/2b = 0{\cdot}79. \tag{3}$$

The wing semispan of the kestrel was measured at 0·338 m and the measured core spacing, D, of 0·51 m gives a value for R′ of 0·76. The agreement is good, well within experimental error. Similarly, a dimensionless core diameter, d/D = 0·17, is given

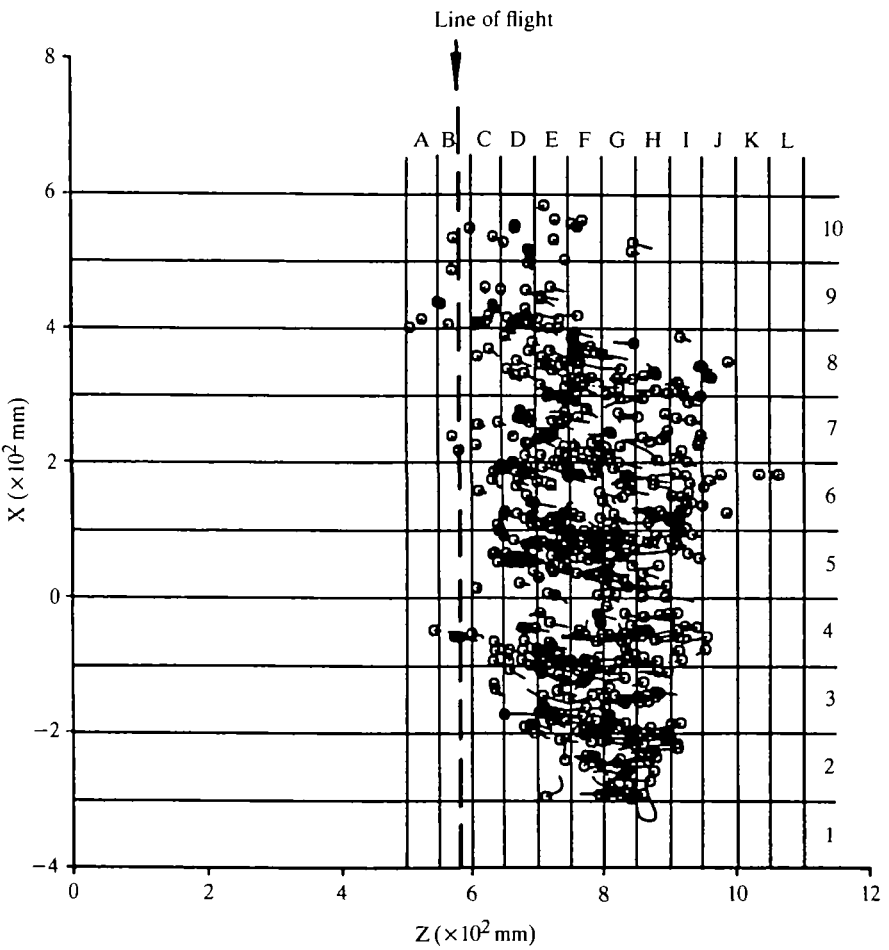

Fig. 4. The wake reconstructed and shown from above, along the Y axis. The leading bubble in each chain is shown by a circle and the length of the trailing tail is proportional to the velocity in the XZ plane. The numbered and lettered sections show the locations of vertical slices taken across and along the wake respectively. The glide path was from top to bottom along the line shown. The back wall is at Z = 0.

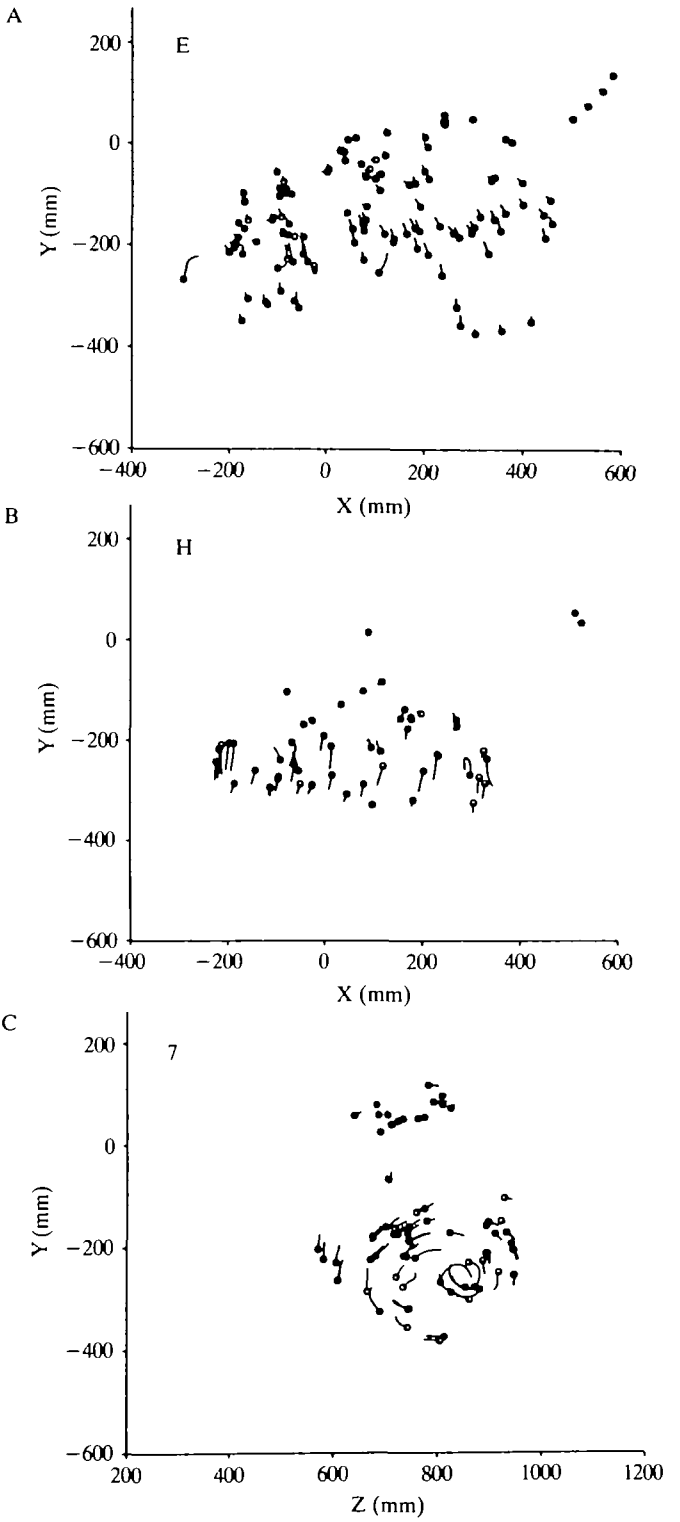

Fig. 5. (A) and (B) are sections E and H from Fig. 4, taken close to the inner and outer boundaries of the vortex core. Similarly, (C) is from section 7 across the wake showing a section close to normal to the long axis of the single vortex visible on this side of the wake.

by lifting line theory, as compared with an experimental value of 0·079/0·51 = 0·15, measured in the kestrel wake. Again, the agreement is better than could reasonably be expected from the accuracy of the experiment.

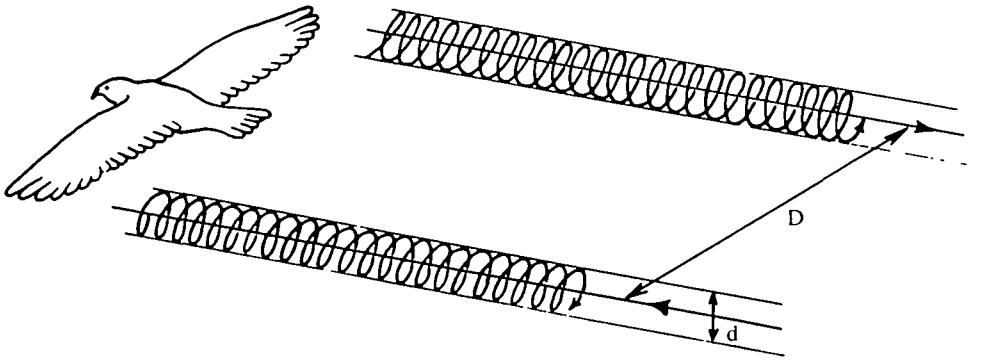

Fig. 6. A schematic view of the vortex wake of a gliding kestrel. The wake element spacing, D, and the core diameter, d, are easily measured.

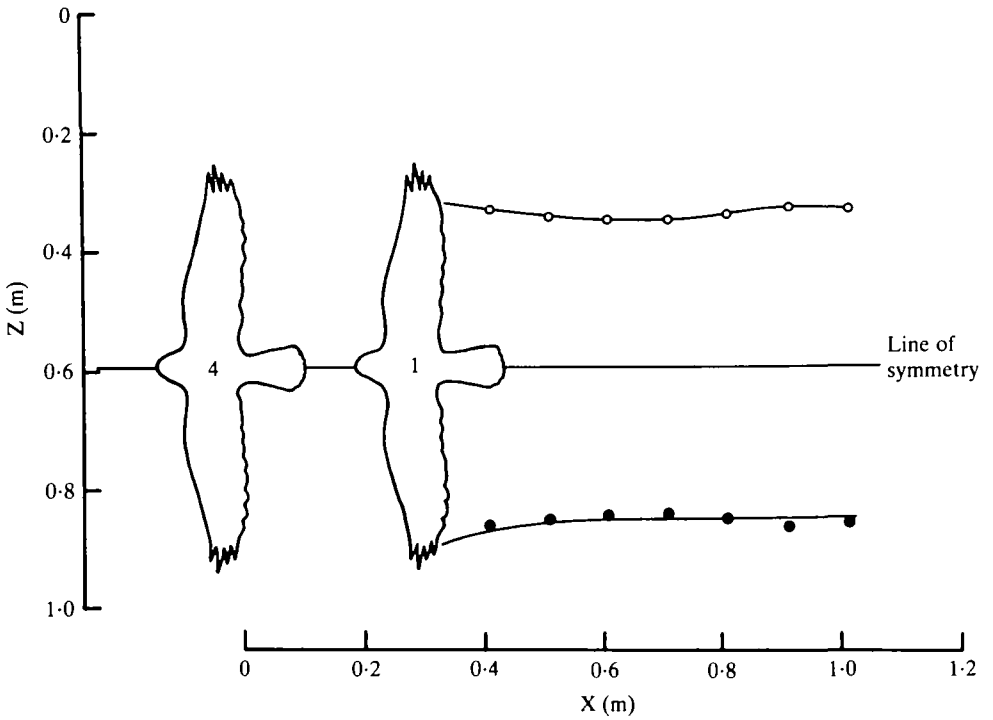

Fig. 7. The XZ location of the trailing vortex from serial reconstructions. The points have been reflected about the line of vertical symmetry but the open circles are connected by a line following an apparent low amplitude oscillation. Curves have been drawn by eye. During the time for the four multiple exposures, the kestrel has moved from position 1 to position 4.

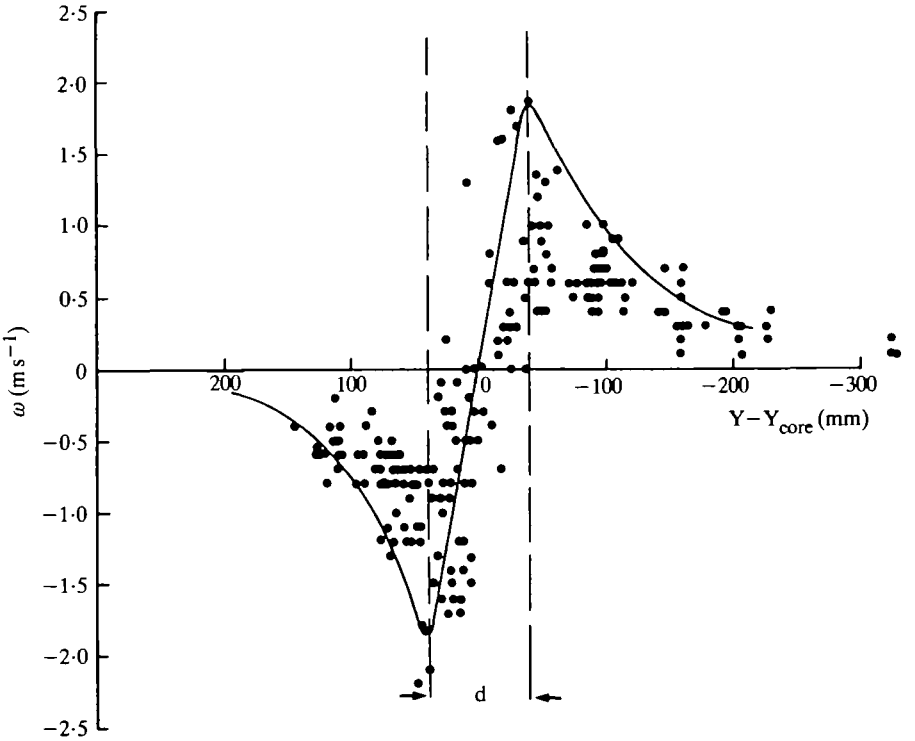

Fig. 8. $w(Y)$ profile along a vertical line running through the vortex core centre. The curve, which has been fitted by eye, was drawn along the edge of the envelope of points to account for the finite thickness of the section in Z. The plot is a collection of data from seven sections down the wake. The estimate of the core diameter, d, probably errs on the large side.

Momentum balance

If the wing is behaving like a classical aerofoil, an approximate check on the expected magnitude of the circulation may be made. Consider an elliptically loaded wing replaced by a lifting line with circulation which, together with the wake vortices, may be represented as a horseshoe vortex lengthening by ∂X in time ∂t (Fig. 9). The rate of change of momentum, $\dot{\mathbf{Q}}$, is

$$\dot{\mathbf{Q}} = \rho\Gamma \cdot 2bR' \cdot \partial X/\partial t, \tag{4}$$

where $\rho = 1{\cdot}205\,\mathrm{kg\,m^{-3}}$ is the air density. If $\dot{\mathbf{Q}}$ is assumed to balance the weight, then,

$$M\boldsymbol{g} = \rho\Gamma \cdot 2bR' \cdot U,$$

and

$$\Gamma = M\boldsymbol{g}/2\rho bR'U, \tag{5}$$

where M is the body mass, $\boldsymbol{g}$ is the gravitational acceleration and $U = \partial X/\partial t$ is the forward flight speed. The terms on the right of equation 5 are all known and for a kestrel of 0·210 kg, gliding at $7\,\mathrm{m\,s^{-1}}$, Γ is calculated as $0{\cdot}476\,\mathrm{m^2\,s^{-1}}$. This compares with a measured value (from equation 1) of $0{\cdot}496\,\mathrm{m^2\,s^{-1}}$. The kestrel appears to be

generating momentum in its wake at a sufficient rate to support its weight, or rather its shallow glide path. Actually, the kestrel will either be losing height, introducing a cosine term into equation 4, or decelerating slowly as it passes the cameras but these corrections should be small and one therefore expects, and finds, a rough balance in forces.

Aerofoil efficiency, lift coefficient

A quantity often quoted in aerodynamics texts and bird flight literature is the efficiency factor '*e*' which may be thought of as simply the lifting efficiency of an aerofoil/wing configuration as compared with the elliptically loaded wing. This value can be inferred directly from the spanwise separation of the wingtip trailing vortices, so

$$e = R'/R'_s, \tag{6}$$

where R'_s is the dimensionless wake element spacing behind an elliptically-loaded wing. From equations 2 and 3, $R'_s = \pi/4$ and,

$$e = 4R'/\pi. \tag{7}$$

Substituting the measured value of R', $e = 0{\cdot}96$.

Assumptions concerning the value of *e* vary in the bird flight literature. Reviewing a range of studies, Greenewalt (1975) drew attention to this wide variation, noting aspects of experimental design which effectively lower the estimated value. He then postulated a rather low value of 0·5–0·7, based on just such data, albeit selected for self-consistency. Withers (1981) reported values ranging from 0·2 to 0·8 based on wind tunnel measurements of fixed wings. These wings were mounted away from the wind tunnel wall, which is likely to increase tip losses considerably, reflected in the low *e* estimates. While the value of *e* reported here is only for one case, the wing/body configuration of the kestrel is not thought to be exceptional in its aerodynamic characteristics. Neither does the value of 0·96 seem improbably high in view of Cone's (1962) finding that *e* may rise above 1·0 in non-planar lifting systems, such as branched wingtips. The value of $e = 0{\cdot}96$ reported here suggests that it might

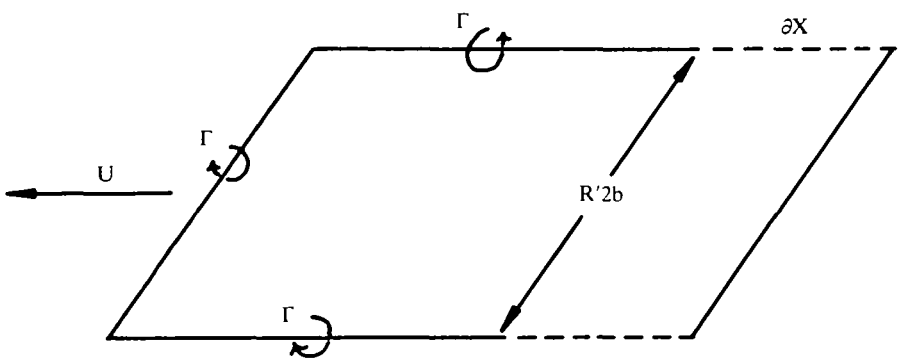

Fig. 9. A wing moving at constant velocity, U, is conceptually replaced by a lifting line of circulation Γ, together with two trailing line vortices of equal circulation. R', wake spacing; b, wing semispan.

normally be taken as close to 1·0, as assumed by Pennycuick (1968), Tucker & Parrott (1970) and Wood (1973), among others.

Assuming, for convenience, that the kestrel is approximately supporting its weight, one can estimate a lift coefficient (C_L) for the kestrel wings in steady flight,

$$C_L = \frac{L}{\frac{1}{2}\rho U^2 S}, \tag{8}$$

where L is the total lift and is assumed to balance the weight, M***g***, and S is the wing area, measured at approximately 0·06 m^2. Thus calculated, $C_L = 1{\cdot}16$. This is quite a moderate value of C_L for an aerofoil at a chord Reynolds number, Re_o, around 4×10^4 ($Re_o = Uc/\nu$, c is the mean chord, ν is the kinematic viscosity of the fluid). For an elliptically loaded wing pair, equation 8 may be expressed as,

$$C_L = \pi b\Gamma_o/SU, \tag{9}$$

where Γ_o is the circulation at the wing centre-line, equal to Γ, the wake vortex circulation, in this case. Substituting the measured value of Γ into equation 9, $C_L = 1{\cdot}25$. The reasonable agreement between the estimates derived from equations 8 and 9 should come as no surprise in view of that found in the previously discussed estimates of Γ, R′ and *e*.

Ground effect

In the case analysed above, the kestrel was gliding about 360 mm above the ground and, given the opportunity (the absence of flashguns on the floor), would have been closer still; in unimpeded flights over a smooth surface the chest feathers were on occasion seen to graze the ground. Ground effect will be significant to any bird flying close to a reasonably smooth surface, solid or water, especially in landing and take-off manoeuvres. Its effect in reduction of induced drag may be modelled as a mitigation of downward induced velocities at the ground due to the presence of a mirror-image vortex system beneath the plane surface. Applying the Biot–Savart law to the horseshoe vortex system of Fig. 9 and its image, McCormick (1979) derived a formula for the ratio of induced drag in ground effect, $C_{D_i(g)}$ to the induced drag in its absence, C_{D_i},

$$C_{D_i(g)}/C_{D_i} = (8h/b)^2/[1 + (8h/b)]^2. \tag{10}$$

Here h is the flying height, b the wing semispan and a typographical error in the original has been corrected. When these two parameters are of the same order of magnitude, this ratio $C_{D_i(g)}/C_{D_i}$ is 0·79, indicating a 21 % reduction in induced drag. With decreasing h, for example to order c, the mean chord length, $C_{Di(g)}/C_{Di} = 0{\cdot}41$. This is a substantial decrease in induced drag and should be measurable in an experiment where the kestrel is allowed to glide over an obstacle-free surface. This might be arranged by suspending the flashguns from the ceiling rather than lying them on the floor as in this experiment. At a flying height, $h = 0{\cdot}360$ m, $C_{Di(g)}/C_{Di} = 0{\cdot}80$ and the ground effect might be considered significant but not dominant; its likely effect would be to reduce the deceleration required to maintain a

level or shallow glide path. This has been discussed in some detail by Blake (1983). Overall, the potential importance of ground effect is clear, although it has been neglected in the analysis reported here on the grounds that the calculated values of R', e and C_L are not likely to be greatly affected. These assumptions could be tested in an experiment conducted along the lines suggested above.

The aerodynamics of a kestrel in steady gliding flight seem to be well described by classical aircraft theory and a steady-state lifting line analysis of an elliptically loaded wing pair should provide accurate estimates of both the drag forces on the wings and the induced velocities in the wake. This is an encouraging basis on which to construct a general model of bird flight, but it is not immediately obvious whether these tenets may be retained in the flapping case. The following paper uses similar methods to examine the same kestrel in medium-speed flapping flight.

The author would like to thank Dr C. J. Pennycuick, who was academic supervisor during the course of this research, and who read an early version of the manuscript. Thanks are also due to Dr J. M. V. Rayner, for valuable advice and discussion, and Dr K. D. Scholey who performed the vital role of operator 1 in all experiments. The financial support of the Science and Engineering Research Council is gratefully acknowledged.

REFERENCES

BLAKE, R. W. (1983). Mechanics of gliding in birds with special reference to the influence of the ground effect. *J. Biomechanics* **16**, 649–654.

CONE, C. D. (1962). The theory of induced lift and minimum induced drag of nonplanar lifting systems. *NASA TR-139*.

GREENEWALT, C. H. (1975). The flight of birds. *Trans. Am. Phil. Soc.* **65**, 4.

LAN, C. E. (1979). The unsteady quasi-vortex-lattice method with applications to animal propulsion. *J. Fluid Mech.* **93**, 747–765.

MCCORMICK, B. W. (1979). *Aerodynamics, Aeronautics and Flight Mechanics*. New York: Wiley.

MILNE-THOMPSON, L. M. (1966). *Theoretical Aerodynamics*. New York: Dover.

NORBERG, U. M. (1979). Morphology of the wings, legs and tail of three coniferous forest tits, the goldcrest, and the treecreeper in relation to locomotor pattern and feeding station selection. *Proc. R. Soc. Ser.* B **287**, 132–165.

PENNYCUICK, C. J. (1968). A wind-tunnel study of gliding flight in the pigeon *Columba livia*. *J. exp. Biol.* **49**, 509–526.

PENNYCUICK, C. J. (1969). The mechanics of bird migration. *Ibis* **111**, 525–556.

PENNYCUICK, C. J. (1971*a*). Gliding flight of the White-Backed Vulture, *Gyps africanus*. *J. exp. Biol.* **55**, 13–38.

PENNYCUICK, C. J. (1971*b*). Control of gliding angle in Ruppell's Griffon Vulture *Gyps ruppellii*. *J. exp. Biol.* **55**, 39–46.

PENNYCUICK, C. J. (1975). Mechanics of flight. In *Avian Biology*, vol. 5 (ed. D. S. Farner, J. R. King & K. C. Parkes). London: Academic Press.

PENNYCUICK, C. J. (1978). Fifteen testable predictions about bird flight. *Oikos* **30**, 165–176.

PENNYCUICK, C. J. (1982). The flight of petrels and albatrosses (Procellariiformes), observed in South Georgia and its vicinity. *Phil. Trans. R. Soc. Ser.* B **300**, 75–106.

PHLIPS, P. J., EAST, R. A. & PRATT, N. H. (1981). An unsteady lifting line theory of flapping wings with application to the forward flight of birds. *J. Fluid Mech.* **112**, 97–125.

RAYNER, J. M. V. (1979*a*). A vortex theory of animal flight. II. The forward flight of birds. *J. Fluid Mech.* **91**, 731–763.

RAYNER, J. M. V. (1979*b*). A new approach to animal flight mechanics. *J. exp. Biol.* **80**, 17–54.

SPEDDING, G. R., RAYNER, J. M. V. & PENNYCUICK, C. J. (1984). Momentum and energy in the wake of a pigeon (*Columba livia*) in slow flight. *J. exp. Biol.* **111**, 81–102.

TORRE-BUENO, J. R. & LAROCHELLE, J. (1978). The metabolic cost of flight in unrestrained birds. *J. exp. Biol.* **75**, 223–229.

TUCKER, V. A. (1971). Flight energetics in birds. *Am. Zool.* **11**, 115–124.

TUCKER, V. A. (1973). Bird metabolism during flight: evaluation of a theory. *J. exp. Biol.* **58**, 689–709.

TUCKER, V. A. & PARROTT, G. C. (1970). Aerodynamics of gliding flight in a falcon and other birds. *J. exp. Biol.* **52**, 345–367.

WITHERS, P. C. (1981). An aerodynamic analysis of bird wings as fixed aerofoils. *J. exp. Biol.* **90**, 143–162.

WOOD, C. J. (1973). The flight of albatrosses (a computer simulation). *Ibis* **115**, 244–256.